**Proceedings of ASME/DSCC 2014**
**ASME 2014 Dynamic Systems and Control Conference**
**October 22-24, 2014, San Antonio, USA**

**DSCC2014-5963**

# SIMULTANEOUS CONTROL OF AN ANKLE-FOOT PROSTHESIS MODEL USING A VIRTUAL CONSTRAINT

**Akshay Nanjangud***
Locomotor Control Systems Laboratory
Department of Mechanical Engineering
University of Texas at Dallas
Richardson, TX 75080
Email: akshay.nanjangud@utdallas.edu

**Robert D. Gregg**†
Locomotor Control Systems Laboratory
Departments of Bioengineering and Mechanical Engineering
University of Texas at Dallas
Richardson, TX 75080
Email: rgregg@utdallas.edu

## ABSTRACT

*Amputee locomotion can benefit from recent advances in robotic prostheses, but their control systems design poses challenges. Prosthesis control typically discretizes the nonlinear gait cycle into phases, with each phase controlled by different linear controllers. Unfortunately, real-time identification of gait phases and tuning of controller parameters limit implementation. Recently, biped robots have used phase variables and virtual constraints to characterize the gait cycle as a whole. Although phase variables and virtual constraints could solve issues with discretizing the gait cycle, the virtual constraints method from robotics does not readily translate to prosthetics because of hard-to-measure quantities, like the interaction forces between the user and prosthesis socket, and prosthesis parameters which are often altered by a clinician even for a known patient. We use the simultaneous stabilization approach to design a low-order, linear time-invariant controller for ankle prostheses independent of such quantities to enforce a virtual constraint. We show in simulation that this controller produces suitable walking gaits for a simplified amputee model.*

*Address all correspondence to this author.

†Robert D. Gregg, IV, Ph.D., holds a Career Award at the Scientific Interface from the Burroughs Wellcome Fund. This work was also supported by the Eunice Kennedy Shriver National Institute of Child Health & Human Development of the National Institutes of Health under Award Number DP2HD080349. The content is solely the responsibility of the authors and does not necessarily represent the official views of the NIH.

## INTRODUCTION

The fields of prosthetics [1,2] and orthotics [3,4] are beginning to benefit from recent advances in the field of robotics for the purpose of restoring mobility after lower-limb amputation or stroke. Such wearable robotic devices possess the potential of improving the quality of life for individuals with physical impairments. However, critical obstacles in the control methodologies employed in these devices limit their clinical use. One such hurdle is the time and effort necessary to tune the control system to a particular individual. This usually arises because an individual's gait cycle is discretized into several discrete "phases" with each phase having its own control model [5,6]. In addition to this, multi-joint prostheses have independent control models for each joint. It requires a team of clinicians and researchers multiple days to tune, by trial and error, several parameters of the control system of an above-knee powered prosthesis to an individual's gait cycle [6]. There is also the additional challenge of real-time distinction and identification of each phase of gait, which varies from individual to individual. This difficulty in distinguishing the phases of gait translates into the control system struggling to "keep up" with the rapidly occurring gait cycle.

The challenges posed by discretizing the gait cycle into phases can be partially addressed by borrowing ideas from recent successes in biped robot locomotion. To generate stable walking gaits in biped robots, a "phase variable" is used to continuously represent the phase of gait, which leads to "virtual constraints" that characterize gait kinematics as a whole [7,8] instead of discretizing the gait cycle into pieces. For prosthesis control system

design, a phase variable can be viewed as a mechanical representation of an individual's progression through a gait cycle, with the advantage that a single variable continuously parametrizes the entire gait cycle with no need for discretization. This idea has been used with some success in the design of control systems for above-knee prostheses [9, 10]. The drawback of this approach is that the control input to the prosthesis is largely dependent on the accuracy of the dynamical model of the prosthesis coupled to the human, the measurements of the prosthesis states, and the loads exerted by the subject on the prosthesis socket. In this way, modeling and measurement inaccuracies pose challenges with regard to clinical viability of such control systems.

Although both approaches of designing control systems for prostheses and orthoses have drawbacks, they have certain merits as well. One employs linear controllers to control the gait which would be easy to implement, if not for the many discrete phases of gait. The other uses a virtual constraint based on a continuous parametrization of the gait's phase to characterize the entire gait cycle. This constraint when enforced by a nonlinear controller is known to produce suitable walking gaits in amputees [11]. Output Proportional-Derivative (PD) control has been used as a linear approximation of this nonlinear controller but the PD control gains are sensitive to model parameters [11]. All this inspires the question: Can linear controllers be used to enforce virtual constraints for an ankle prosthesis to produce suitable walking gaits in amputees regardless of variations in model parameters? In this work we design such a controller. Our controller is a linear time-invariant (LTI), single-input single-output (SISO) transfer function of only second-order, and requires sensor measurements of only the prosthesis states.

We begin by reviewing a nonlinear continuous-time ankle prosthesis model from [12] for which we design a control system. Then we explain a virtual constraint, which uses the center of pressure (COP) as a phase variable, that our controller must enforce to produce suitable walking gaits. Next, we proceed to linearizing the nonlinear prosthesis model and the virtual constraint to obtain an LTI plant. From this linearization we define a finite set of plants to be stabilized in order to account for uncertainties in various prosthesis and human subject parameters. Then we design a second-order, SISO, LTI controller that simultaneously stabilizes all these plants. Finally, we simulate the prosthesis control system with the full biped to show a symmetric stable walking gait. In the section on simulations, we also compare the results from the feedback linearizing controller designed in [12].

## A NONLINEAR MODEL OF AN ANKLE-FOOT PROSTHESIS

In this section we review a nonlinear dynamical model of an ankle prosthesis in a manner pertinent to our control system design. Refer to [12] for more details.

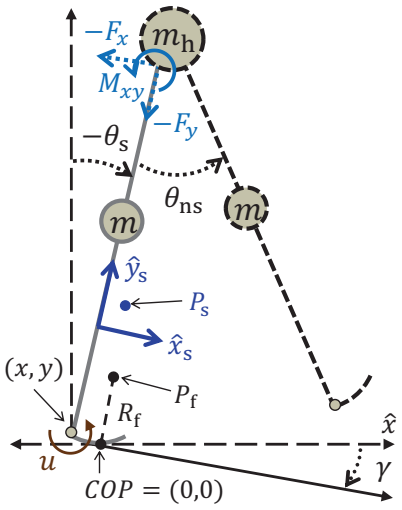


Figure 1. Kinematic model of a compass-gait biped with rocker feet [12].

We employ a simple dynamical model with no knees to reduce the state-space dimensions of the model. In the late stance period the function of the human ankle is plantarflexion of the foot to propel the individual forward. In the swing period the ankle merely lifts the foot to facilitate ground clearance. Therefore, our objective is to design a control system that produces suitable walking gaits in human subjects with emphasis on the control of a prosthetic ankle bearing the human subject weight during stance. The planar biped model shown in Fig. 1 has a hip joint, and ankle joints with constant-curvature rocker feet. These rocker feet approximate the deformation of human feet during walking [13]. The stance leg is shown in solid gray to represent a prosthesis attached to the subject's body (shown in dashed black) at the hip. First, only the stance leg is modeled for the control system design. Then the full biped model of the human subject wearing the prosthesis is simulated to show periodic locomotion.

We now review the continuous dynamics of the ankle prosthesis. It is modeled as a kinematic chain with respect to the COP. After reviewing the prosthesis dynamics we explain a kinematic foot constraint, which forces the COP to move along the rocker foot. This kinematic constraint is not to be confused with the virtual constraint that mimics the human effective shape. We conclude this modeling section with a discussion of this virtual constraint.

### Dynamics

In this section we review a continuous time dynamical model of the ankle prosthesis in the stance period. A simplifying assumption in the modeling is that the ankle is defined at the heel. Using the rocker foot shown in Fig. 1, we assume rolling point contact between the foot and ground. Since a rolling contact point has zero velocity at any instant [14], we can treat this

contact point as stationary and model movement of the kinematic chain around it, i.e., the COP is defined at the inertial reference frame. With the COP as the origin, Cartesian coordinates $x, y$ represent the position of the ankle center with respect to the COP. The stance leg angle is defined with respect to the vertical and is denoted by $\theta_s$. Then the configuration of the stance leg, viz., the ankle prosthesis, is denoted as $q = (x, y, \theta_s)^T$; the state of the system is given by the vector $z = (q^T, \dot{q}^T)^T$, where $\dot{q} = (\dot{x}, \dot{y}, \dot{\theta}_s)^T$ denotes the prosthesis joint velocities. During the continuous single-support stance period, the state trajectory evolves according to the set of differential equations

$$M(q)\ddot{q} + C(q,\dot{q})\dot{q} + N(q) + A^T(q)\lambda = \tau, \tag{1}$$

where $M$ is the inertia matrix, $C$ is the matrix of Coriolis terms, $N$ is the vector of gravitational torques, $A$ is the kinematic foot constraint vector for the rocker foot, and $\lambda$ is the Lagrange multiplier providing the forces to enforce the kinematic foot constraint. The vector of external forces $\tau = Bu + J^T(q)F$ is composed of actuator torques and interaction forces $F = [F_x, F_y, M_{xy}]^T$ from the subject's body, respectively. Ankle actuation is provided by the scalar torque input $u$ and mapped into the leg's coordinate system by $B = [0, 0, 1]^T$. For more details on the interaction force vector $F$ and Jacobian $J$ refer to [12].

## Kinematic Foot Constraint

We now review the kinematic constraint which forces the COP to move along the rocker foot as in [12]. Recall that the COP is defined as the origin. The rocker foot is modeled by constraining the heel point $(x, y)$ to an arc that has radius $R_f$ with center of rotation $P_f$ and intersecting the COP. The center of rotation $P_f$ is defined in a moving reference frame such that the vector between $P_f$ and the COP is always normal to the ground with radius $||P_f - COP|| = R_f$. Define

$$\rho = \gamma + 2\arcsin(\frac{d}{2R_f}), \tag{2}$$

where $\gamma$ is the slope angle of the walking surface, and $d = \sqrt{x^2 + y^2}$ is the distance between the COP and the heel. Then the kinematic constraint is given in model coordinates by $k(q) = 0$, where

$$k(q) = (x - R_f\sin(\rho))^2 + (y + R_f\cos(\rho))^2 - R_f^2. \tag{3}$$

Following the method in [12, 15], the constraint vector $A = \nabla_q k$ and Lagrange multiplier $\lambda = \widehat{\lambda} + \widetilde{\lambda}u + \bar{\lambda}F$ are derived, where

$$\begin{aligned}
\widehat{\lambda} &= (AM^{-1}A^T)^{-1}(\dot{A}\dot{q} - AM^{-1}(C\dot{q} + N)),\\
\widetilde{\lambda} &= (AM^{-1}A^T)^{-1}AM^{-1}B,\\
\bar{\lambda} &= (AM^{-1}A^T)^{-1}AM^{-1}J^T.
\end{aligned} \tag{4}$$

It is highlighted here that the rocking constraint $k(q) = 0$ only restricts the motion of the COP to be along the foot, whereas the virtual constraint discussed in the following section characterizes the pendular trajectory of the stance leg about the ankle-foot complex.

## Virtual Constraint

To design an ankle-foot prosthesis control system we use the method of virtual constraints to mimic the effective shape of the human ankle-foot complex for walking. Since amputees often struggle to adapt to varying conditions like gait speed and shoe symmetry [16], we use the invariant property of effective shape explained in [17, 18] as a virtual constraint. This shape characterizes how the ankle moves as the COP travels from heel to toe during walking. For the model used in this work, where the heel and ankle are combined for simplicity, the resulting trajectories of the stance leg angle $\theta_s$ differ from the ankle trajectories seen in the biomechanics literature. Reviewed here is a virtual constraint from [12], which when satisfactorily enforced by control action mimics the effective shape of the stance leg even though the joints modeled are not analogous to the physiological joints.

The effective shape is the COP trajectory mapped into a shank-based reference frame, which is shown with axes $\hat{x}_s, \hat{y}_s$ in Fig. 1. Able-bodied humans have effective shapes specific to activities such as walking or stationary swaying [18], and each shape can be characterized by the curvature of the COP trajectory with respect to a point $P_s = (X_s, Y_s)^T$ attached to the shank reference frame. This can be expressed as the coordinate-free distance relationship

$$||P_s - COP|| = R_s, \tag{5}$$

where the radius of curvature $R_s$ is a constant for walking. At heel strike the COP is co-linear with the dynamical model's stance leg and the condition in Eqn. (5) is necessarily satisfied, so the $Y_s$-component of $P_s$ is given by $Y_s = \sqrt{R_s^2 - X_s^2}$. In model coordinates Eqn. (5) is given by the virtual holonomic constraint $h(q) = 0$ where

$$\begin{aligned}
h(q) = {} & (x + X_s\cos(\theta_s) - Y_s\sin(\theta_s))^2 + \\
& (y + X_s\sin(\theta_s) + Y_s\cos(\theta_s))^2 - R_s^2.
\end{aligned} \tag{6}$$

The virtual constraint defined by Eqn. (6) represents the desired behavior of the prosthetic ankle. Our attempt is to enforce this nonlinear virtual constraint with a SISO, LTI controller.

## LINEAR TIME-INVARIANT PLANT FOR THE ANKLE-FOOT PROSTHESIS MODEL

To design an LTI controller for the continuous system in Eqn. (1), we first linearize this nonlinear model of the ankle prosthesis. A fixed point of the system is

$$x = y = \theta_s = \dot{x} = \dot{y} = \dot{\theta}_s = 0, \tag{7}$$

which corresponds to the prosthesis in a vertically upright position. We develop a linear approximation of the ankle prosthesis model at this unstable fixed point. We begin by defining the states

$$z_1 = x, \quad z_2 = y, \quad z_3 = \theta_s, \quad z_4 = \dot{x}, \quad z_5 = \dot{y}, \quad z_6 = \dot{\theta}_s, \tag{8}$$

and inputs $u$, $F_x$, $F_y$ and $M_{xy}$. Then the nonlinear system in Eqn. (1) can be rewritten as a set of first-order ordinary differential equations of the form

$$\dot{z} = f(z) + g(z)\hat{u}, \tag{9}$$

where $z = [z_1, z_2, z_3, z_4, z_5, z_6]^T$ and $\hat{u} = [u, F_x, F_y, M_{xy}]^T$. Linearizing the system in Eqn. (9) at the equilibrium point in Eqn. (7), we get LTI state-space equations of the form

$$\dot{z} = Az + B\hat{u}, \tag{10}$$

where

$$A = \begin{bmatrix} 0_{3\times3} & I_{3\times3} \\ A_3 & 0_{3\times3} \end{bmatrix}, \quad B = \begin{bmatrix} 0_{3\times4} \\ B_2 \end{bmatrix}, \tag{11}$$

with

$$A_3 = \frac{mg\ell}{2I_x}\begin{bmatrix} 0 & 0 & \frac{\ell}{2} \\ 0 & 0 & 0 \\ 0 & 0 & 1 \end{bmatrix}, \quad B_2 = \begin{bmatrix} \frac{\ell}{2I_x} & \frac{1}{m} - \frac{\ell^2}{4I_x} & 0 & \frac{\ell}{2I_x} \\ 0 & 0 & \frac{1}{m} & 0 \\ \frac{1}{I_x} & \frac{-\ell}{2I_x} & 0 & \frac{1}{I_x} \end{bmatrix}, \tag{12}$$

where $m$, $\ell$ and $I_x$ are the mass, length and moment of inertia of the ankle prosthesis, respectively, and $g$ is the acceleration due to gravity taken to be 9.81 m-s$^{-2}$. The pair $(A, B)$ is fully controllable. However, the interaction forces $F_x, F_y$ and $M_{xy}$ do not represent control inputs from the ankle prosthesis, but rather from the human subject. Define

$$B_u := [0, 0, 0, \frac{\ell}{2I_x}, 0, \frac{1}{I_x}]^T, \tag{13}$$

which represents the input-matrix for the control torque from the ankle prosthesis. The Popov-Belevitch-Hautus Test (see [19]) shows the pair $(A, B_u)$ to be controllable with respect to all states except $z_5 = \dot{y}$. This state corresponds to the vertical velocity of the ankle/heel center with respect to the COP. It is noted that the prosthesis can influence this state through the controllable states in the foot contact constraint $k(q) = 0$, with $k(q)$ as given by Eqn. (3). In addition to this, the human subject can also exert control over this state through the interaction forces $F_x, F_y$ and $M_{xy}$.

To obtain an LTI plant $G(s) = \tilde{C}(sI - A)^{-1}B_u$ we need an output-matrix $\tilde{C}$. For this we use the virtual constraint $h(q) = 0$ with $h(q)$ in Eqn. (6) as the output function. We have earlier stated that driving the virtual constraint to zero would mimic walking in able-bodied humans. So the function $h(q)$ can be thought of as an output that is to be zeroed by the LTI controller we design. To this effect we derive an output-matrix $\tilde{C}$ by linearizing $h(q)$ about the equilibrium point in Eqn. (7); we get

$$\tilde{C} = [2X_s,\ 2Y_s,\ 0,\ 0,\ 0,\ 0]. \tag{14}$$

Then the LTI plant of the ankle prosthesis is

$$G(s) = \frac{\ell X_s}{I_x(s^2 - \frac{mg\ell}{2I_x})}. \tag{15}$$

## LINEAR CONTROLLER DESIGN FOR THE LINEARIZED PROSTHESIS PLANT

In this section we design a controller for the LTI plant $G(s)$ in Eqn. (15). It is known that clinicians often make adjustments to the length and weight of the prosthesis to satisfy the changing demands of the human subject, which means the prosthesis parameters are far from being fixed quantities. Moreover, the quantity $X_s$ in the LTI plant $G(s)$ is a human subject parameter normalized by the subject's height, and it varies for different slopes of walking surface [17]. Therefore, our objective is to design a controller that gives due consideration to these uncertainties. Our approach to accounting for these is by defining several different LTI plants for different values of prosthesis and subject parameters and then designing *just one, common* controller that stabilizes all these plants. Such an approach of stabilizing a finite number of LTI plants with the use of one controller is called

Simultaneous Stabilization (see [20]), which we merge with the method of virtual constraints. Along similar lines a compass-gait biped model with point feet was simultaneously stabilized to account for parameter uncertainties in [21].

Define the parameters

$$k := \frac{\ell X_s}{I_x}, \; p^2 = \frac{mg\ell}{2I_x}, \tag{16}$$

which are not fixed quantities for the reasons just explained. Recall that $m$, $\ell$ and $I_x$ are physical parameters of the prosthesis, while $X_s$ is a human subject parameter. Then the LTI plant in Eqn. (15) becomes

$$G(s) = \frac{k}{(s^2 - p^2)}. \tag{17}$$

At this point our objective is to design a SISO, LTI controller that stabilizes $G(s)$ even when $k$ and $p$ are not accurately known.

Based on values for an average human subject used in [12], we define a nominal plant $G_o$ with $k_o$ and $p_o$ given by $\ell = 0.865$ m, $X_s = 0.005$ m, $I_x = 0.2$ kg-m$^2$, and $m = 13.5$ kg. We now define more plants $G_1, G_2, \ldots, G_{11}$ within physiological ranges from [12] in the following manner: First, in order to account for uncertainties in the measurement of $\ell$, we define $G_1$, $G_2$, and $G_3$ when $\ell$ equals 0.7, 0.8 and 0.9 m, respectively, keeping the values of other parameters the same as that in the nominal plant $G_o$. Next, to account for the uncertainty in $X_s$, we define $G_4$ and $G_5$ when $X_s$ equals 0.1 and 0.3 m, respectively, maintaining the values of all other parameters as in $G_o$. In similar fashion, we define $G_6$ and $G_7$ when $I_x$ equals 0.1 and 0.3 kg-m$^2$, respectively, $G_8$ and $G_9$ when $m$ equals 12.5 and 14.5 kg, respectively. To illustrate that more than one parameter can be varied at a time, we define $G_{10}$ when $\ell = 0.75$ m, $X_s = 0.015$ m and $I_x = 0.15$ kg-m$^2$, and define $G_{11}$ when $\ell = 0.95$ m, $X_s = 0.025$ m, $I_x = 0.25$ kg-m$^2$ and $m = 15$ kg. Note that there is no limit to the number of such plants that can be simultaneously stabilized using the design procedure we describe. Our goal now is to design one SISO, LTI controller that stabilizes all plants in the set $\mathcal{G} = \{G_o, G_1, G_2, \ldots, G_{11}\}$.

We now design a simultaneously stabilizing controller based on the design procedure developed in [22]. Let $g_c = 2$, $z_c = 3$. For each $G_j$ in $\mathcal{G}$ define

$$\Psi_j(s) := s[\frac{1}{(s+g_c)(s+z_c)} G_j^{-1} k_o - \frac{k_o}{k_j}], \tag{18}$$

$$\Phi_j(s) := s[(1 + \frac{s}{\alpha(s+g)(s+z)} G_j^{-1} k_o)^{-1} \\ (\frac{g}{\alpha(s+g_c)(s+z_c)} G_j^{-1} k_o - 1)]. \tag{19}$$

We choose $\alpha = 120$ and $\beta = 120$ such that

$$\alpha > \max_{G_j \in \mathcal{G}} ||\Psi_j(s)||, \tag{20}$$

$$\beta > \max_{G_j \in \mathcal{G}} ||\Phi_j(s)||. \tag{21}$$

Then the SISO, LTI controller that simultaneously stabilizes all plants in $\mathcal{G}$ is

$$C(s) = \frac{\alpha\beta(s+g_c)(s+z_c)}{k_o s(s+g+\beta)} \\ = \frac{10^5(3.364s^2 + 16.82s + 20.19)}{s(s+122)}. \tag{22}$$

This controller is only second-order and provides integral-action. Also highlighted is the fact that there are infinitely many controllers that stabilize the set $\mathcal{G}$ for different values of $g_c, z_c > 0$, and $\alpha$ and $\beta$ satisfying the conditions in (20) and (21), respectively. In addition to these, the controller $C(s)$ is independent of the interaction forces exerted by the human subject on the prosthesis, which is not the case for the partial feedback linearizing controller derived in [12].

Note that there is no limit in the choice and number of plants $G_o$, $G_1$, $G_2$, ... ,$G_{11}$. More such plants can be generated and simultaneously stabilized by choosing different values for the prosthesis and subject parameters. Since there is no limit to the number of plants that can be simultaneously stabilized, doing so with more plants takes greater care of the uncertainties in prosthesis and subject parameters.

## SIMULATING THE FULL BIPED WITH ANKLE PROSTHESIS

The simultaneous controller $C(s)$ in Eqn. (22) is now simulated with a nonlinear hybrid biped model. We cover two cases in our simulations: downslope walking with $\gamma = 0.0075$ radians, and flat ground walking with $\gamma = 0$.

First, we simulate the case of the biped walking down a slope with $\gamma = 0.0075$ radians. In this case the biped has an existing passive walking gait; we add our ankle prosthesis control system to the biped and observe how well this controller enforces the virtual constraint $h(q) = 0$ to achieve biomimetic walking. This is also studied to draw performance comparisons with the partial feedback linearizing controller designed in [12].

Next we simulate the full biped walking on level ground, i.e., when the slope $\gamma$ of the walking surface is zero. This case was not covered in the feedback linearizing design in [12]. Since the biped does not have a passive walking gait on flat surface, we add an input at the hip of the human subject to move appropriately the human subject's swing leg to generate a walking gait. The input we provide at the hip is based on the idea of controlled symmetries and passive walking, which is discussed in [23]. The method of controlled symmetries exploits passive gaits in bipeds to generate a 'pseudo-passive' gravity based human like gait input, which is conjectured to represent the energy-efficient walking gaits in humans.

Now we briefly explain a full biped model from [12] before discussing the results of our simulations. The configuration vector of the full biped is denoted by $\hat{q} = (q^T, \theta_{ns})^T$, where $\theta_{ns}$ is the hip (i.e., non-stance) angle as defined in Fig. 1. The biped's dynamics during single support are governed by a differential equation of the form (1) until the swing foot contacts the ground, which initiates the transition into the next step cycle. We define a function $H_\gamma(\hat{q})$ to give the height of the heel of the swing foot above ground with slope angle $\gamma$, so heel strike occurs when the state trajectory intersects the switching surface $G = \{\hat{q} \mid H_\gamma(\hat{q}) = 0\}$. The subsequent double-support transition is modeled as an instantaneous impact event with a perfectly plastic (inelastic) collision as in [7]. The state trajectory is therefore subjected to the impact map $\Delta$ (which also changes the values of $\theta_s, \theta_{ns}$ to re-label the stance and swing legs) in the hybrid dynamical system:

$$\begin{aligned} \hat{M}(\hat{q})\ddot{\hat{q}} + \hat{C}(\hat{q},\dot{\hat{q}})\ \dot{\hat{q}} + \hat{N}(\hat{q}) + \hat{A}^T(\hat{q})\hat{\lambda} = \tau \ \text{ for } \hat{q} \notin G \\ (\hat{q}^+, \dot{\hat{q}}^+) = \Delta(\hat{q}^-, \dot{\hat{q}}^-) \ \text{ for } \hat{q} \in G, \end{aligned} \quad (23)$$

where the superscripts $+/-$ denote the post- and pre-impact states, respectively, the input vector $\tau$ is given by

$$\tau = \begin{bmatrix} 0 & 0 \\ 0 & 0 \\ 1 & 0 \\ 0 & 1 \end{bmatrix} \begin{bmatrix} u \\ u_h \end{bmatrix}, \quad (24)$$

where $u$ represents the control input from the prosthesis, and $u_h$ represents the input at the human hip from controlled symmetries. The input $u_h$ is zero for downslope walking. For level ground walking it is given by

$$u_h = 0.5mg\ell(\sin(\theta_s + \theta_{ns}) - \sin(\theta_s + (\gamma_{\text{act}} - \gamma_{\text{vir}}) + \theta_{ns})), \quad (25)$$

where $\gamma_{\text{act}}$ is the slope of walking surface on which a walking gait is to be achieved, and $\gamma_{\text{vir}}$ is a choice of virtual slope of the walking surface. For our full biped model we take $\gamma_{\text{vir}} = 0.0325$ rad. Since we wish to achieve flat ground walking, we must have $\gamma_{\text{act}} = 0$ rad. For full details on the other terms associated with the full biped model in Eqn. (23), see [12]. The state of the full biped system is given by the vector $\hat{z} = (\hat{q}^T, \dot{\hat{q}}^T)^T$. Since the controller $C(s)$ in Eqn. (22) is second-order, it adds two further states to the full biped system. The controller $C(s)$ is written in state-space form as

$$\begin{bmatrix} \dot{x}_{c_1} \\ \dot{x}_{c_2} \end{bmatrix} = \begin{bmatrix} -122 & 0 \\ 1 & 0 \end{bmatrix} \begin{bmatrix} x_{c_1} \\ x_{c_2} \end{bmatrix} + \begin{bmatrix} 1 \\ 0 \end{bmatrix} e(t),$$

$$u = [-3935800 \ \ 2019000] \begin{bmatrix} x_{c_1} \\ x_{c_2} \end{bmatrix} + 336400\, e(t), \quad (26)$$

where $x_{c_1}$ and $x_{c_2}$ are the states of the controller, $e(t)$ is the error in the virtual constraint to be zeroed, i.e., $e(t) = 0 - h(q(t))$, and $u$ is the ankle torque generated by the ankle prosthesis controller on the stance leg to help produce stable walking gaits. When simulating we determine the error $e(t)$ from the nonlinear form of $h(q)$ as in Eqn. (6) although the simultaneous controller $C(s)$ is designed for $h(q)$ linearized at the fixed point in Eqn. (7).

When simulating the full biped model in Eqn. (23) in closed-loop with the control system in Eqn. (26), we only consider walking gaits corresponding to stable periodic solutions of the hybrid biped model. Such solutions define isolated orbits in the state space known as *hybrid limit cycles*, which correspond to fixed points of the Poincarè return map $P : G \to G$. We verify exponential stability of periodic walking gaits by ensuring the eigenvalues of the discritized Poincarè return map, linearized about its fixed point corresponding to the periodic solution, lie within the unit circle. This procedure is explained in [7].

## Downslope Walking

In this section we compare the performance of the LTI simultaneous controller designed in this work to the feedback linearizing controller designed in [12]. A PD controller is also designed in [12]. Since our simultaneous controller outperforms that PD controller, we only compare our simultaneous controller with the feedback linearizing controller. Broadly speaking, the performances of the simultaneous controller and the feedback linearizing controller in simulation are almost evenly matched for downslope walking with the slope of walking surface $\gamma$ being 0.0075 radians.

Note that for this slope the biped exhibits a passive gait and the only input to the biped is at the prosthesis, i.e., $u_h = 0$ in Eqn. (24), and $u$ is either the input given by the LTI, simultaneous controller in Eqn. (26), or the input given by the feedback linearizing controller in [12], as the case may be.

Figures 2 and 3 show the angular positions of the biped with feedback linearizing control and simultaneous control, respectively, for three consecutive steps. Since our modeling simplification assumes the heel and ankle to coincide, the angle $\theta_s$ is not the physiological ankle angle seen in the biomechanics literature. Hence, it is not expected that $\theta_s$ match those typical ankle trajectories seen in biomechanics data. Figures 4 and 5, compare the phase portraits for both controllers. It can be seen from Figures 6 and 7 that the COP moves almost just as far from the ankle for both controllers. In Fig. 8 we see that the simultaneous controller exerts lower torque than the feedback linearizing controller. However, the enforcement of the virtual constraint from the feedback linearizing controller is better than the simultaneous controller as can be inferred from Fig. 9.

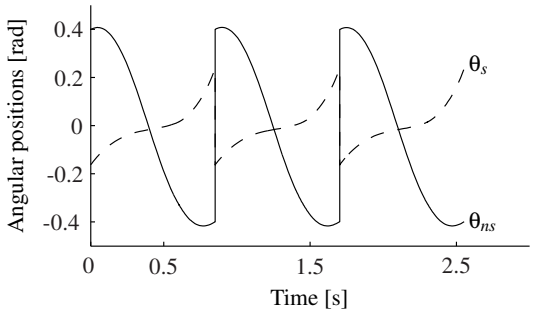


Figure 2. ANGULAR POSITIONS OF THE FEEDBACK LINEARIZATION CONTROLLED BIPED WITH PROSTHESIS WALKING DOWNSLOPE.

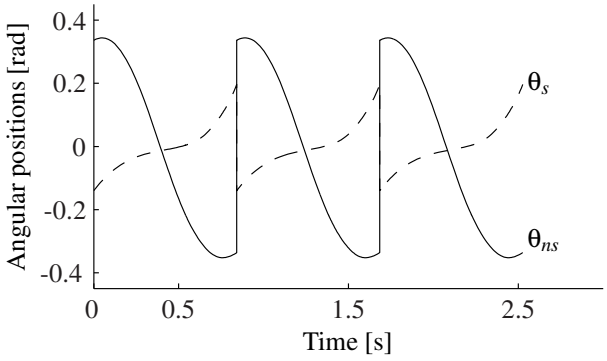


Figure 3. ANGULAR POSITIONS OF THE SIMULTANEOUSLY CONTROLLED BIPED WITH PROSTHESIS WALKING DOWNSLOPE.

When comparing the two controllers the important factors are the ankle torques experienced by the human subject and the enforcing of the virtual constraint $h(q) = 0$. The simultaneous

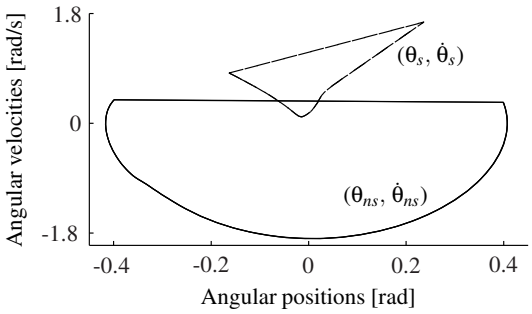


Figure 4. PHASE PORTRAIT OF THE FEEDBACK LINEARIZATION CONTROLLED BIPED WITH PROSTHESIS WALKING DOWNSLOPE.

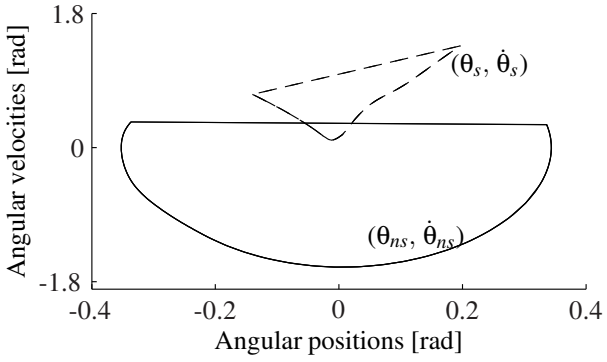


Figure 5. PHASE PORTRAIT OF THE SIMULTANEOUS CONTROLLED BIPED WITH PROSTHESIS WALKING DOWNSLOPE.

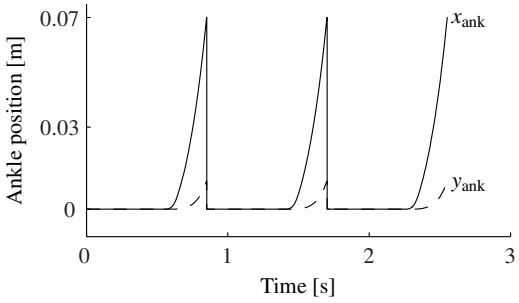


Figure 6. ANKLE POSITIONS OF THE FEEDBACK LINEARIZATION CONTROLLED BIPED WITH PROSTHESIS WALKING DOWNSLOPE.

controller exerts lower ankle torques on the human subject than the feedback linearizing controller. This also reduces expectations from the actuators in the prosthesis when the simultaneous controller is implemented. However, the enforcement of the virtual constraint is done better by the feedback linearizing design, which should be no surprise because of the linear nature of the proposed simultaneous controller. It is again noted that the feedback linearizing controller, which needs real-time measurement of the interaction forces $F_x$, $F_y$ and $M_{xy}$ and a model of the pros-

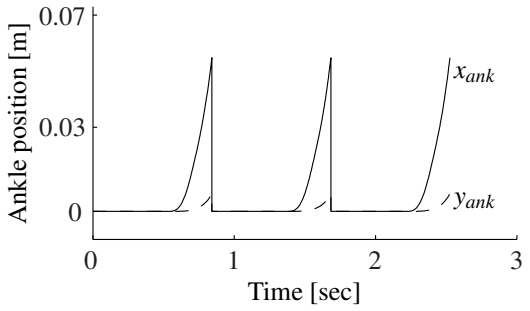


Figure 7. ANKLE POSITIONS OF THE SIMULTANEOUS CONTROLLED BIPED WITH PROSTHESIS WALKING DOWNSLOPE.

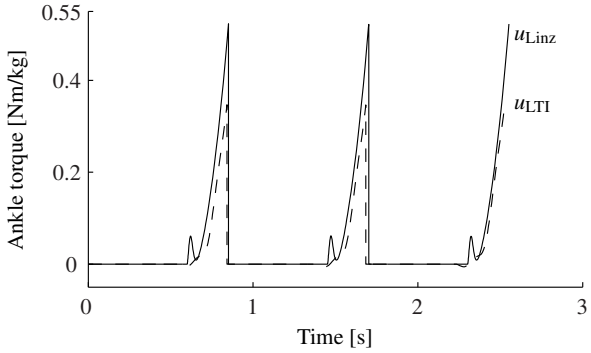


Figure 8. ANKLE TORQUES FROM THE FEEDBACK LINEARIZING AND SIMULTANEOUS CONTROLLED BIPED WITH PROSTHESIS WALKING DOWNSLOPE.

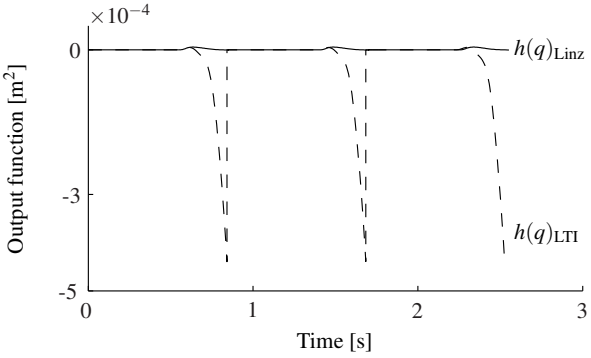


Figure 9. VIRTUAL CONSTRAINT ENFORCEMENT COMPARISON FOR FEEDBACK LINEARIZING AND SIMULTANEOUS CONTROLLERS.

thesis properties, is harder to implement than the simultaneous controller.

## Flat Ground Walking

In this section we present the results for flat ground walking of the full biped with ankle prosthesis. This case has not been studied in [12]. Since the biped does not possess a passive gait for $\gamma = 0$, we use $u_h$ as shown in Eqn. (25). Figures 10, 11, 12, 13 and 14 show the angular positions, phase portrait, ankle positions, ankle torques and the output function $h(q)$, respectively, for the simultaneously controlled biped walking on flat ground.

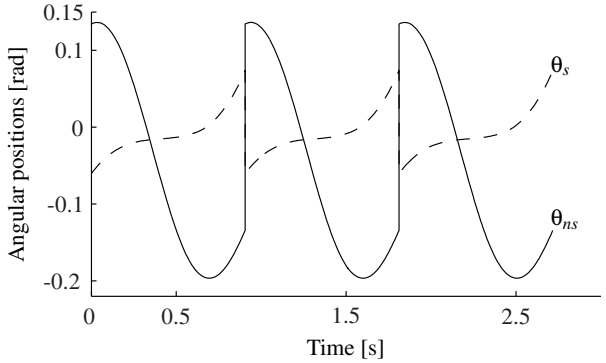


Figure 10. ANGULAR POSITIONS OF THE SIMULTANEOUS CONTROLLED BIPED WITH PROSTHESIS WALKING ON FLAT GROUND.

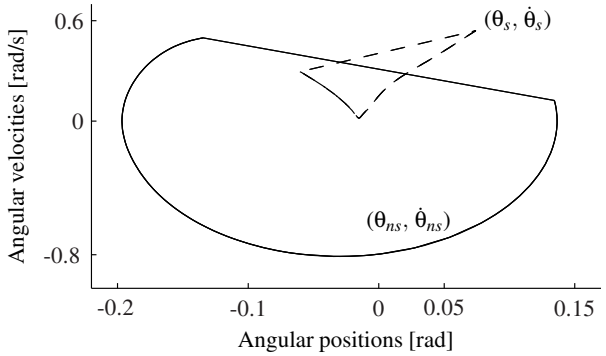


Figure 11. PHASE PORTRAIT OF THE SIMULTANEOUS CONTROLLED BIPED WITH PROSTHESIS WALKING ON FLAT GROUND.

The simulations show us that the ankle prosthesis controller designed using the simultaneous stabilization approach produces flat ground walking given a suitable input at the human subject's hip for motion of the swing leg. As one would expect, Fig. 13 suggests that flat ground walking requires greater ankle torque than downslope walking that permits passive gaits for the biped. Figure 12 suggests that the COP does not move as much on flat

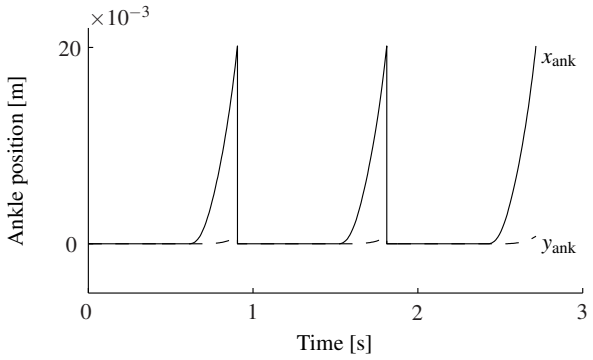


Figure 12. ANKLE POSITIONS OF THE SIMULTANEOUS CONTROLLED BIPED WITH PROSTHESIS WALKING ON FLAT GROUND.

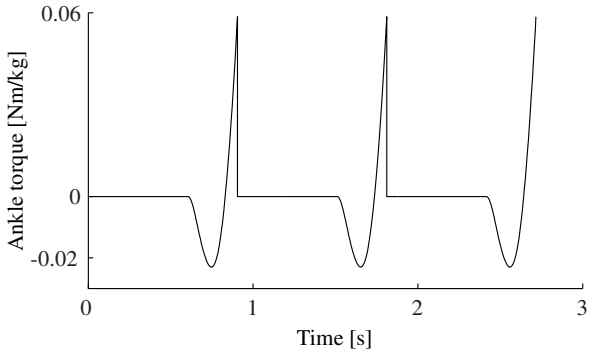


Figure 13. ANKLE TORQUE FROM THE SIMULTANEOUS CONTROLLED BIPED WITH PROSTHESIS WALKING ON FLAT GROUND.

ground walking as it does for downslope walking, which again is in line with our intuition. Since the output function $h(q)$ has very small values across the gait cycle in Fig. 14, our simultaneous controller seems to maintain the human effective shape for walking on flat surfaces.

## CONCLUSIONS

Despite recent developments in technology, lower-limb prosthesis control systems design faces several challenges. Prosthesis control systems have traditionally relied on a time-varying linear control scheme that struggles to "keep up" with respect to the phases of a rapidly occurring gait cycle. In this work, ideas such as phase variables and virtual constraints from the field of bipedal robotics were exploited to design a SISO, LTI controller which does not have to adapt for different phases of a gait cycle. In addition, the closed loop system formed by the human subject and the prosthesis is autonomous in nature. This controller also accounts for uncertainties in prosthesis and human subject parameters, and relies on sensor measurements of only the prosthesis states. Most importantly, this linear controller satisfactorily enforces a nonlinear virtual constraint to maintain the human effective shape for biomimetic walking of amputees with ankle prostheses. Since the linear controller employs high gains, lower values of gain may be explored in implementation on an ankle prosthesis. In future, higher degree of freedom models of transfemoral amputees using prostheses will be considered for simultaneous control.

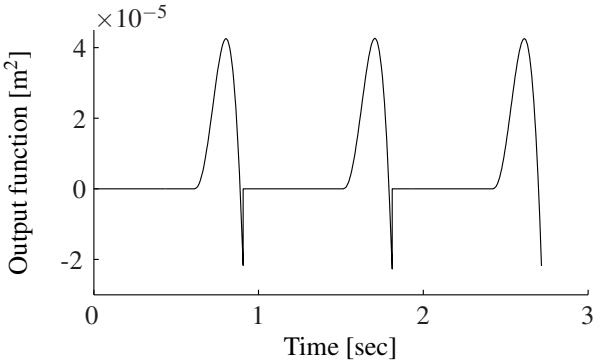


Figure 14. VIRTUAL CONSTRAINT ENFORCEMENT FOR THE SIMULTANEOUS CONTROLLED BIPED WITH PROSTHESIS WALKING ON FLAT GROUND.

## REFERENCES


[1] Sup, F., Bohara, A., and Goldfarb, M., 2008. "Design and control of a powered transfemoral prosthesis". *International Journal of Robotics Research,* **27**(2), pp. 263–273.

[2] Sup, F., Varol, H., and Goldfarb, M., 2011. "Upslope walking with a powered knee and ankle prosthesis: Initial results with an amputee subject". *IEEE Transactions on Neural Systems and Rehabilitation Engineering,* **19**(1), pp. 71–78.

[3] Shorter, K. A., Hsiao-Wecksler, E. T., Kogler, G. F., Loth, E., and Durfee, W. K., 2011. "A portable powered ankle-foot-orthosis for rehabilitation". *Journal of NeuroEngineering and Rehabilitation,* **48**(4), pp. 459–472.

[4] Boehler, A. W., Hollander, K. W., Sugar, T. G., and Shin, D., 2008. "Design, implementation and test results of a robust control method for a powered ankle foot orthosis (AFO)". In IEEE International Conference on Robotics and Automation, pp. 2025–2030.

[5] Eilenberg, M., Geyer, H., and Herr, H., 2010. "Control of a powered ankle–foot prosthesis based on a neuromuscular model". *IEEE Transactions on Neural Systems and Rehabilitation Engineering,* **18**(2), pp. 164–173.

[6] Simon, A., Fey, N., Finucane, A., Lipschutz, R., and Hargrove, L., 2013. "Strategies to reduce the configuration time for a powered knee and ankle prosthesis across multiple ambulation modes". In IEEE International Conference on Rehabilitation Robotics.

[7] Westervelt, E. R., Grizzle, J. W., Chevallereau, C., Choi, J. H., and Morris, B., 2007. *Feedback Control of Dynamic Bipedal Robot Locomotion*. CRC Press, New York, NY.

[8] Sreenath, K., Park, H. W., Poulakakis, I., and Grizzle, J. W., 2011. "A compliant hybrid zero dynamics controller for stable, efficient and fast bipedal walking on MABEL". *International Journal of Robotics Research,* **30**(9), pp. 1170–1193.

[9] Gregg, R. D., and Sensinger, J. W., 2013. "Biomimetic virtual constraint control of a transfemoral powered prosthetic leg". In American Control Conference, pp. 5702–5708.

[10] Gregg, R. D., Lenzi, T., Fey, N. P., Hargrove, L. J., and Sensinger, J. W., 2013. "Experimental effective shape control of a powered transfemoral prosthesis". In IEEE International Conference on Rehabilitation Robotics.

[11] Gregg, R. D., Lenzi, T., Hargrove, L. J., and Sensinger, J. W., 2014. "Virtual constraint control of a powered prosthetic leg: From simulation to experiments with transfemoral amputees". *IEEE Transactions on Robotics*. under review.

[12] Gregg, R., and Sensinger, J., 2014. "Towards biomimetic virtual constraint control of a powered prosthetic leg". *IEEE Transactions on Control Systems Technology,* **22**(1), pp. 246–254.

[13] Adamczyk, P. G., Collins, S. H., and Kuo, A. D., 2006. "The advantages of a rolling foot in human walking". *Journal of Experimental Biology,* **209**(20), pp. 3953–3963.

[14] Hibbeler, R. C., 2012. *Engineering Mechanics: Dynamics*, 13 ed. Prentice Hall, Upper Saddle River, NJ.

[15] Murray, R. M., Li, Z., and Sastry, S. S., 1994. *A Mathematical Introduction to Robotic Manipulation*. CRC Press, Boca Raton, FL.

[16] Smith, D. G., Michael, J. W., and Bowker, J. H., 2004. *Atlas of Amputations and Limb Deficiencies: Surgical, Prosthetic, and Rehabilitation Principles*. American Academy of Orthopaedic Surgeons, Rosemont, IL.

[17] Hansen, A., and Childress, D., 2010. "Investigations of roll-over shape: Implications for design, alignment, and evaluation of ankle-foot prostheses and orthoses". *Disability & Rehabilitation,* **32**(26), pp. 2201–2209.

[18] Hansen, A., and Wang, C., 2010. "Effective rocker shapes used by able-bodied persons for walking and fore-aft swaying: Implications for design of ankle-foot prostheses". *Gait & Posture,* **32**(2), pp. 181–184.

[19] Kailath, T., 1980. *Linear Systems*. Prentice-Hall, Englewood Dliffs, NJ.

[20] Vidyasagar, M., 1985. *Control System Synthesis: A Factorization Approach*. MIT Press, Cambridge, MA.

[21] Nanjangud, A., and Gregg, R. D., 2014. "Simultaneous control of the compass-gait biped to maintain symmetric gait across all mass ratios". In American Control Conference, pp. 5490–5495.

[22] Gündeş, A., and Nanjangud, A., 2012. "Simultaneous stabilization and constant reference tracking of LTI, MIMO systems". *Asian Journal of Control,* **15**(4), pp. 1001–1010.

[23] Spong, M. W., and Francesco, B., 2005. "Controlled symmetries and passive walking". *IEEE Transactions on Automatic Control,* **50**(7), pp. 1025–1031.